Am J Nucl Med Mol Imaging 2023;13(6):279-288
www.ajnmmi.us /ISSN:2160-8407/ajnmmi0153740

Case Report

Malignant melanoma of gastrointestinal tract on ^{18}F-FDG PET/CT: three case reports

Wenpeng Huang[1*], Yongkang Qiu[1*], Xiaoyan Xiao[2], Liming Li[2], Qi Yang[1], Jianbo Gao[2], Lei Kang[1]

[1]Department of Nuclear Medicine, Peking University First Hospital, Beijing 100034, China; [2]Department of Radiology, The First Affiliated Hospital of Zhengzhou University, Zhengzhou 450052, Henan, China. [*]Equal contributors.

Received October 1, 2023; Accepted December 21, 2023; Epub December 25, 2023; Published December 30, 2023

Abstract: Primary malignant melanoma most frequently occurs in the skin. Melanoma affecting the gastrointestinal (GI) tract has been substantiated for lesions occurring in the esophagus, stomach, small bowel, and anorectum through multiple published reports, given the presence of melanocytes in these areas. Nevertheless, owing to the exceedingly low incidence of this disease, reports on its clinical features are few, and treatment approaches lack standardization. In this study, we present three cases of GI melanoma with imaging manifestations, emphasizing the pivotal role of ^{18}F-FDG PET/CT in staging for GI melanoma. Establishing a definitive diagnosis of primary GI melanoma necessitates the exclusion of the possibility of metastasis from more prevalent primary sites. Advancements in molecular imaging technologies and the development of novel tracers provided significant promising methods for enhancing the diagnosis and management of melanoma, contributing to improved patient outcomes and overall disease management.

Keywords: Malignant melanoma, gastrointestinal tract, stomach, intestine, ^{18}F-FDG PET/CT, case report

Introduction

Global incidence of malignant melanoma has risen significantly over the past two decades [1]. Melanoma is an epithelial cancer originating from melanocytes, which can be found in various tissue types, including the eye, oral cavity, nasopharynx, anus, urinary tract, and vagina; however, it overwhelmingly arises from the skin [2-4]. Less frequently encountered are melanomas, both primary and metastatic, within the gastrointestinal (GI) tract. GI melanocytes originate from melanoblastic cells of the neural crest, migrating to the GI mucosa, especially in the esophagus and anorectal region [5-7]. Metastatic lesions typically stem from primary cutaneous or ocular lesions, with the majority metastasizing to the small bowel [8]. GI melanoma might be misdiagnosed due to its lower frequency and concealed location. Previous studies indicate 5-year survival rates for colorectal melanoma ranging from 4.3% to 17.4%; esophageal and gastric melanoma exhibit even shorter survival rates [9]. Generally, outcomes for patients with mucosal melanoma are worse compared to those with cutaneous melanoma, partly attributed to delayed examinations and diagnoses among GI melanoma patients. Given that the majority of GI melanomas have a metastatic origin, comprehensive physical examinations and imaging studies are imperative to differentiate them from primary cutaneous or ocular melanomas. While ^{18}F-FDG PET/CT is employed for staging cutaneous melanoma, there is limited literature addressing its application in the management of gastrointestinal melanoma.

This report highlights the role of FDG PET/CT in imaging and staging for GI melanoma. A definitive diagnosis of primary GI melanoma can be established after ruling out the possibility of it being a metastasis from other, more common primary sites.

Case presentation

Case 1

A 43-year-old man presented with low back pain 7 months ago and fever up to 39°C 5

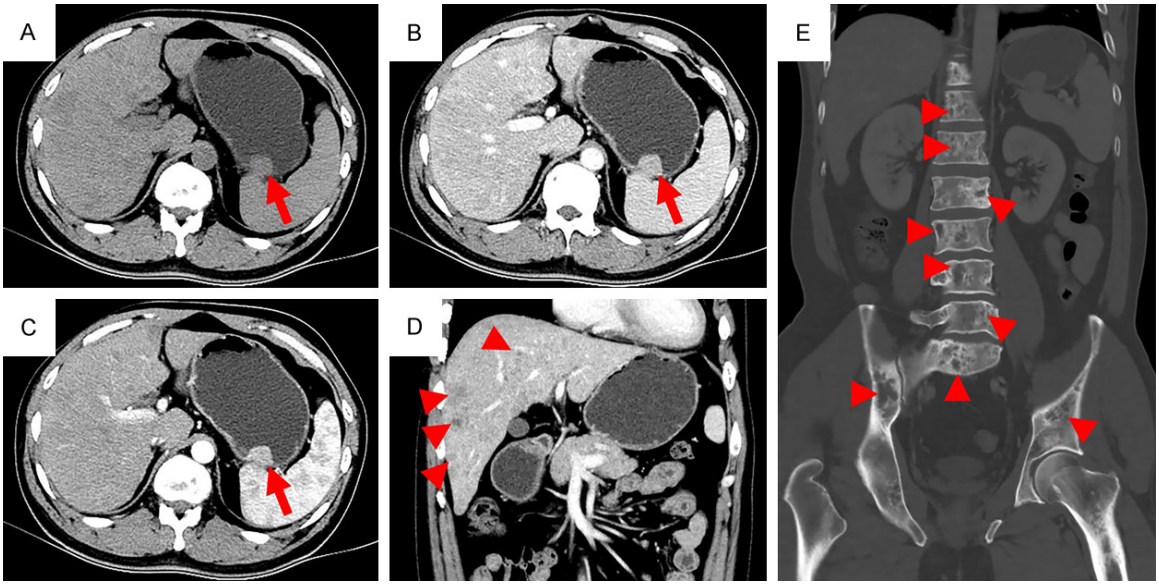

Figure 1. Computed tomography (CT) images of gastric malignant melanoma. A-C. The transverse images in the plain, arterial, and venous phases depicted polypoid soft tissue nodules projecting into the gastric cavity, exhibiting CT attenuation of 40, 92, and 87 HU, respectively (long arrows). These nodules displayed well-defined margins and uniform, marked enhancement. D. In the coronal venous phase image, multiple metastases in the liver were observed (arrowheads). E. In the coronal image (bone window), multiple metastases in the vertebrae and pelvis were visualized (arrowheads).

months ago. The patient was previously healthy with no history of tumor or familial genetic disease. The patient underwent CT examination which revealed a soft tissue nodule measuring approximately 2.5 cm × 1.9 cm on the greater curvature side of the fundus of the stomach, with a CT attenuation of 45 HU on plain scanning (**Figure 1A**), and marked homogeneous enhancement in the arterial and venous phases with a CT attenuation of 87 HU and 45 HU, respectively (**Figure 1B**, **1C**), and multiple metastases in the liver, spine, and pelvis were also found (**Figure 1D**, **1E**). For further staging, the patient underwent ^{18}F-FDG PET/CT. PET MIP image revealed FDG-avid lesions in both lungs, the liver, and multiple bones throughout the body (**Figure 2A**). Increased FDG uptake was observed in the gastric body lesions (SUVmax = 10.4). Multiple soft-tissue density nodules in both lungs exhibited increased FDG uptake (SUVmax = 12.6), the largest of which measured approximately 1.8 cm × 1.8 cm. Hilar lymph nodes on both sides displayed increased FDG uptake (SUVmax = 19.6). Localized thickening of the right pleura, along with heightened FDG uptake (SUVmax = 13.4). Moreover, multiple hypodense lesions were detected in the liver (SUVmax = 16.1), the largest of which measured about 1.6 cm × 2.4 cm. Multiple bone disruptions were observed in the sternum, bilateral clavicles, bilateral scapulae, multiple vertebrae and their attachments, multiple ribs bilaterally, and proximal femurs bilaterally, all displaying heightened FDG uptake (SUVmax = 45.7) (**Figure 2B-F**).

The patient underwent a gastroscopic pathological biopsy, revealing a diffuse proliferation of heterogeneous tumor cells organized in sheets and nested clusters, characterized by intracytoplasmic melanin granules and apparent nuclear atypia (**Figure 3A**). Immunohistochemistry demonstrated positive expression of MelanA, HMB45, S-100, and SOX-10 (**Figure 3B-E**). Additionally, Ki-67 displayed positive staining in 40% of the tumor cells (**Figure 3F**). Consequently, the clinical diagnosis indicated gastric melanoma with multiple metastases. After completing four cycles of chemotherapy using the 'Cisplatin + Temozolomide + Amlotinib' regimen, the patient's response was assessed as stable disease (SD). Subsequently, zoledronic acid was administered to address potential bone metastasis. Unfortunately, the patient succumbed to the illness after a 13-month follow-up period.

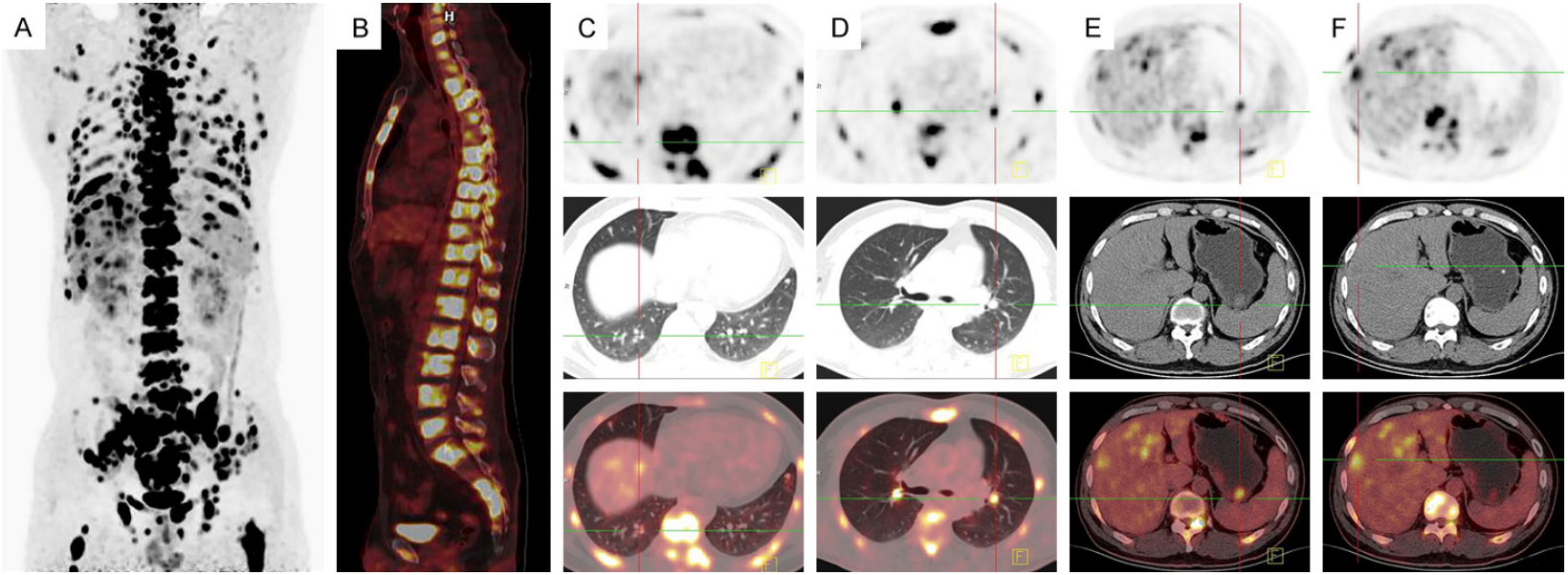

Figure 2. ^{18}F-FDG PET/CT images of gastric malignant melanoma. A. The anteroposterior 3-dimensional maximum intensity projection image (MIP) demonstrated FDG-avid lesions in both lungs, the liver, and multiple bones throughout the body. B. Sagittal fusion image showed multiple bone metastases throughout the body (SUVmax = 45.7). C. The transverse images revealed multiple soft-tissue density nodules in both lungs, which displayed heightened FDG uptake (SUVmax = 12.6), with the largest measuring approximately 1.8 cm × 1.8 cm. D. Hilar lymph nodes on both sides displayed increased FDG uptake (SUVmax = 19.6). E. Elevated FDG uptake was observed in a soft tissue nodule located lateral to the greater curvature of the gastric body (SUVmax = 10.4). F. The transverse images revealed multiple hypodense lesions within the liver, exhibiting a SUVmax of 16.1, with the largest lesion measuring approximately 1.6 cm × 2.4 cm.

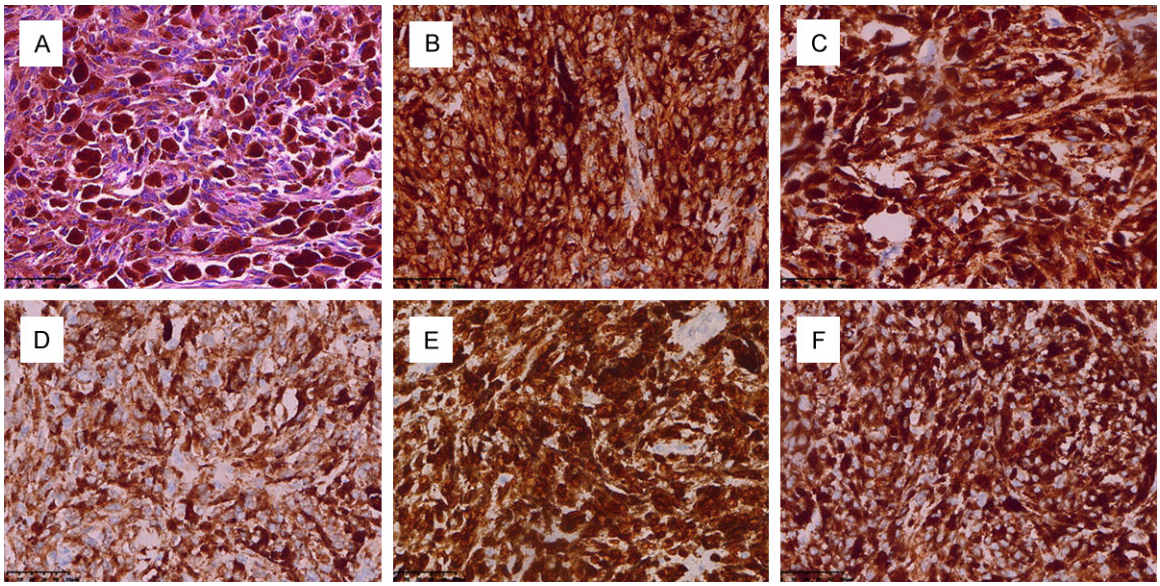

Figure 3. Histopathological and immunohistochemical images of gastric malignant melanoma. (A) Hematoxylin-eosin (HE) staining (magnification ×400) of the lesion revealed a diffuse proliferation of heterogeneous tumor cells organized in sheets and nested clusters, characterized by intracytoplasmic melanin granules and apparent nuclear atypia. Immunohistochemical staining (400×) showed tumor cells were positive for the expression of MelanA (B), HMB45 (C), S-100 (D) and SOX-10 (E). Ki-67 was observed to be positive in 40% of the tumor cells (F).

Case 2

A 38-year-old male was admitted to hospital for recurrent abdominal pain and fever for three months, which could be exacerbated by eating, without hematochezia, vomiting or diarrhea. A contrast-enhanced computed tomography scan of the entire abdomen demonstrated an irregular soft tissue mass with moderately heterogeneous enhancement in the ileum, measuring approximately 10.0 cm × 8.9 cm. The mass exhibited communication with the intestinal lumen and contained gas density (**Figure 4A**, **4B**). Additionally, multiple lymph nodes with enhancement were identified in the mesentery, retroperitoneum, and left perirenal space (**Figure 4C**, **4D**). To clarify the nature of the ileal mass and alleviate the patient's symptoms, the patient underwent ileal mass resection and lymphadenectomy. The postoperative pathology showed the mass invaded the whole layer of the ileal wall with ill-defined borders. The pleomorphic tumor cells formed a papillary pattern and pigmentation was observed in some cells (**Figure 4E**). Immunohistochemical staining with S-100 (**Figure 4F**), Melan A (**Figure 4G**), and HMB-45 (**Figure 4H**) was positive, which supported the diagnosis of melanoma. Given the rarity of primary malignant melanoma of the small intestine, a comprehensive physical examination and ^{18}F-FDG PET/CT were conducted one month after surgery to exclude metastatic ileal melanoma and to stage. No possible primary melanoma lesion was detected on the scalp or skin, oral and nasopharyngeal cavities, or eyes, and the ^{18}F-FDG PET/CT demonstrated no skin lesions with high metabolic activity (**Figure 5A**). Unexpectedly, a mass with elevated FDG uptake measuring 2.7 cm × 3.9 cm was discovered in the middle lobe of the right lung, with a SUVmax of 8.5 (**Figure 5B**). Additionally, lymph nodes with varying degrees of increased FDG uptake were identified in the left supraclavicular, mediastinum, right hilum, mesentery, and retroperitoneum, with a SUVmax of 8.8 (**Figure 5C**, **5D**). Subsequent biopsy of the right lung mass confirmed the presence of metastatic malignant melanoma. By comparing the histological characteristics of the lesions in the ileum and right lung, and taking into account the more conspicuous lesions and metastasis foci in the abdomen, the final diagnosis was determined to be primary malignant melanoma of the ileum with lung and lymph nodes metastasis. The patient underwent four cycles of chemotherapy with the 'Cortisol + Axitinib' regimen, resulting in disease stabilization. The patient is currently under follow-up to monitor their condition.

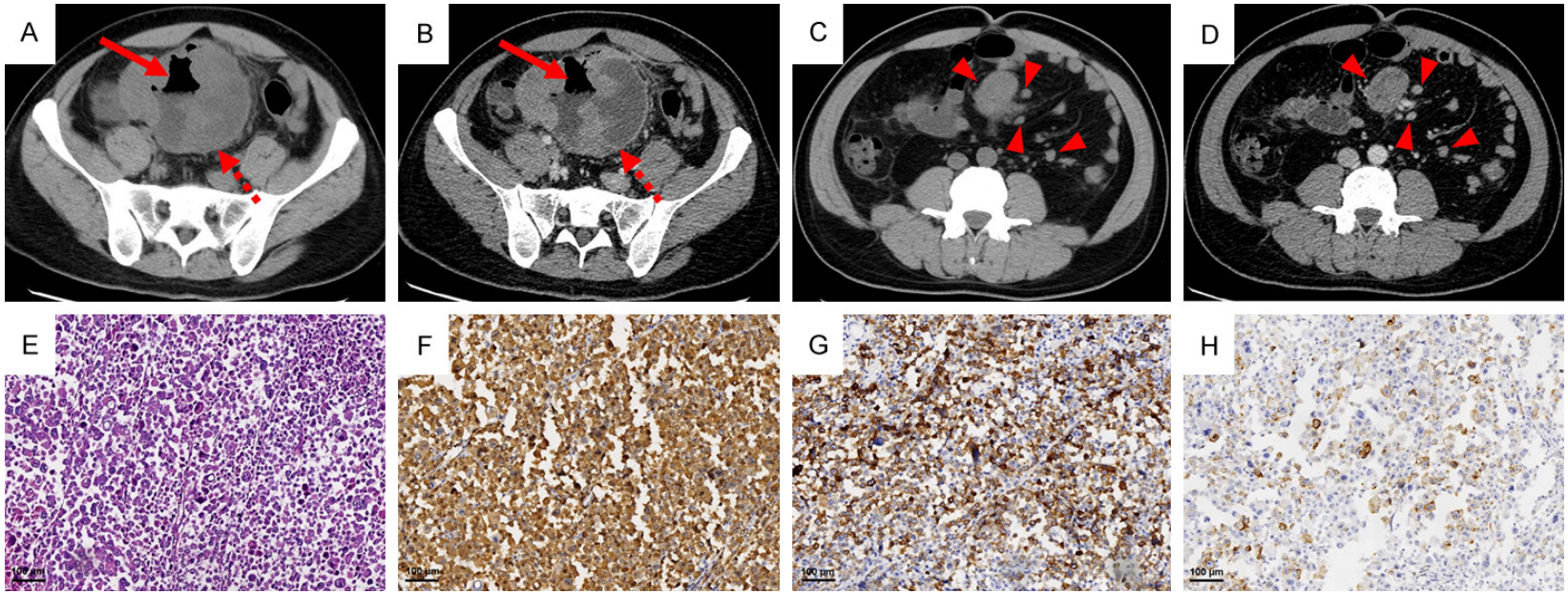

Figure 4. Computed tomography (CT) images, histopathological and immunohistochemical images of ileal melanoma. (A, B) CT demonstrated an irregular soft tissue mass with moderately heterogeneous enhancement in the ileum, measuring approximately 10.0 cm × 8.9 cm (long arrows). The mass exhibited communication with the intestinal lumen and contained gas density (dashed arrows). (C, D) Multiple lymph nodes with enhancement were identified in the mesentery, retroperitoneum, and left perirenal space (arrowheads). (E) The postoperative HE pathology showed the mass invaded the whole layer of the ileal wall with ill-defined borders. The pleomorphic tumor cells formed a papillary pattern and pigmentation was observed in some cells (magnification ×200). Immunohistochemical staining (200×) showed tumor cells were positive for the expression of S-100 (F), MelanA (G), and HMB-45 (H).

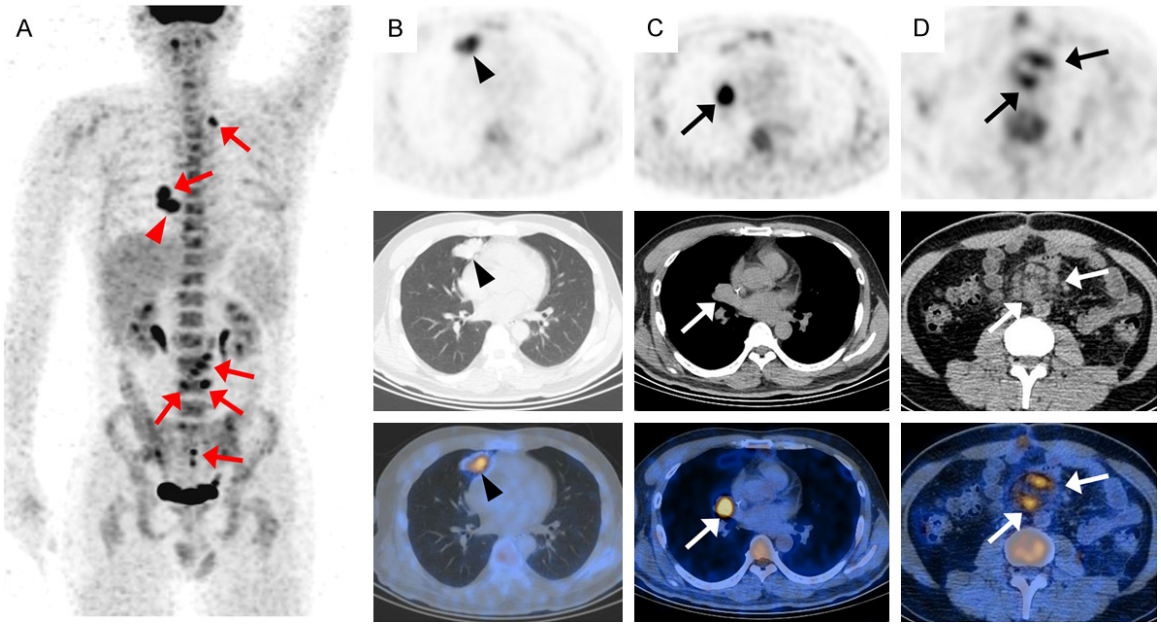

Figure 5. ^{18}F-FDG PET/CT images of ileal melanoma. A. The anteroposterior 3-dimensional maximum intensity projection image (MIP) demonstrated FDG-avid lesions in the right lung (long arrows) and multiple lymph nodes throughout the body (arrowheads). B. A mass with elevated FDG uptake measuring 2.7 cm × 3.9 cm was discovered in the middle lobe of the right lung, with a SUVmax of 8.5. C, D. Lymph nodes with varying degrees of increased FDG uptake were identified in the left supraclavicular, mediastinum, right hilum, mesentery, and retroperitoneum, with a SUVmax of 8.8.

Case 3

A 57-year-old man presented with mucoid black stools, paroxysmal lower and middle abdominal pain, abdominal distension, and vomiting one year ago without any apparent cause. Subsequent CT examination led to the diagnosis of intestinal volvulus. Consequently, he underwent surgical resection, confirming the presence of melanoma. He received high-dose recombinant human interferon α2b as part of his post-surgery treatment. Subsequently, the patient underwent a CT examination, revealing a soft tissue mass measuring approximately 5.7 cm × 7.2 cm × 7.1 cm in the wall of the jejunal tube, displaying marked inhomogeneous enhancement (**Figure 6A**, **6B**). For further staging, the patient underwent ^{18}F-FDG PET/CT. PET MIP image revealed FDG-avid lesions in the jejunal. Inside the mass, heterogeneous FDG uptake was observed with SUVmax of 10.2 (**Figure 6C-E**). The patient then underwent surgical resection, and postoperative pathology and immunohistochemistry confirmed the diagnosis of recurrent melanoma (**Figure 7**). The patient recovered well after surgery and has been followed up for 8 months with no recurrence or metastasis.

Discussion

GI melanoma falls under the category of mucosal melanomas and can manifest in any segment of the digestive tract, either as primary tumors or metastases stemming from cutaneous, ocular, or anal melanomas [13]. Mucosal melanoma represents an exceptionally rare disease, constituting only 1-2% of all melanoma cases, with an incidence rate ranging from 2 to 2.6 cases per 1,000,000 individuals per year [9-12]. However, mucosal melanoma exhibits greater invasiveness and carries a more unfavorable prognosis when compared to melanomas originating in other sites. The concealed growth site and the lack of early typical symptoms of mucosal melanoma, often result in delays in both examination and diagnosis, ultimately contributing to its grim prognosis. The symptoms documented in the literature of GI melanoma, such as dysphagia, abdominal pain, distention, bleeding, obstruction, and intussusception, are non-specific, rendering the diagnostic process challenging [14, 15]. In patients with a history of melanoma who present with persistent, nonspecific symptoms like vague abdominal pain, fatigue, melena, and anemia, suspicion should arise regarding the possibility

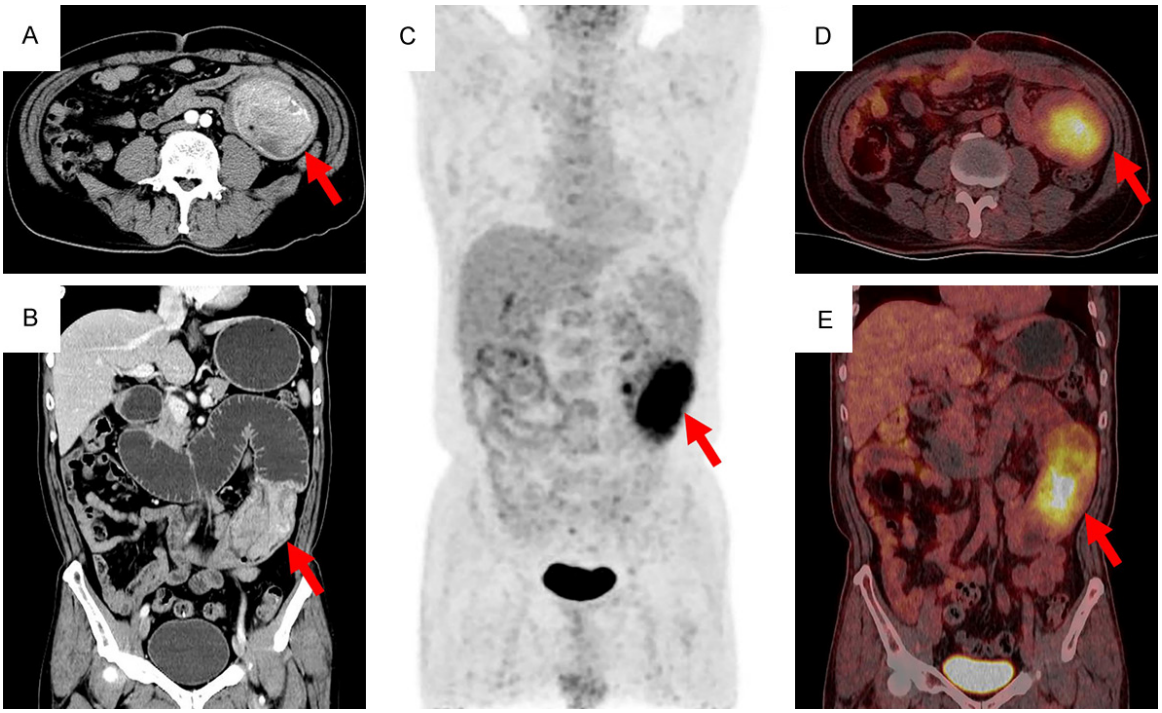

Figure 6. CT images and ^{18}F-FDG PET/CT images of jejunal melanoma. A. The transverse image in the arterial phase shows a CT attenuation of 103 HU for the lesion (long arrows), with a smooth margin. B. Coronal image of the venous phase shows a CT attenuation of 85 HU for the lesion with inhomogeneous marked enhancement. C. The anteroposterior 3-dimensional maximum intensity projection (MIP) image demonstrated FDG-avid lesions in the jejunum (long arrows). D, E. The transverse and coronal fusion image demonstrated heterogeneous FDG uptake with SUVmax of 10.2.

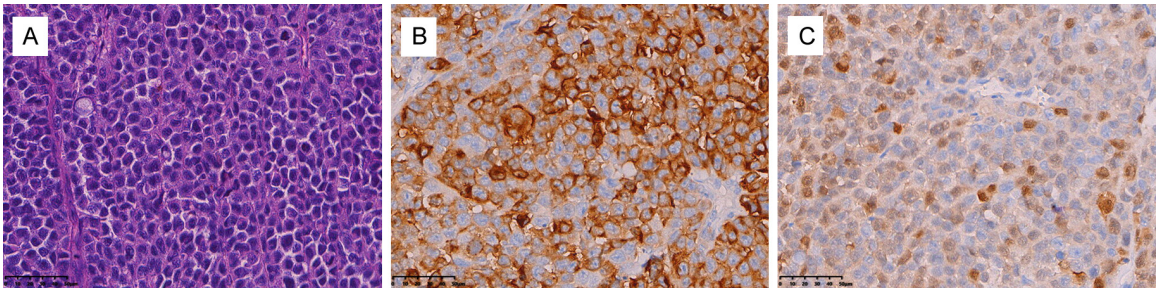

Figure 7. Histopathological and immunohistochemical images of jejunal melanoma. (A) HE staining (magnification ×400) of the lesion revealed heterogeneous tumor cells infiltrating the entire layer of the intestinal wall. Immunohistochemical staining (400×) showed tumor cells were positive for the expression of MelanA (B) and S-100 (C).

of GI tract metastasis, necessitating a thorough diagnostic evaluation from the outset [16, 17].

The pathogenesis of primary GI melanoma primarily revolves around theories related to tumor regression and ectodermal differentiation [18]. Currently, there is a notable absence of evidence-based guidelines for diagnosing primary melanoma in anatomical sites where its occurrence is infrequent. Given the rarity of primary GI melanoma, some propose that melanoma found within the GI tract without a discernible primary lesion could potentially be the result of metastasis from previously existing and spontaneously regressed cutaneous melanoma [15]. The diagnosis of GI melanoma necessitates a pathologic examination. Under microscopic scrutiny, tumor cells often exhibit diffuse distribution in sheets, showcasing a

diverse range of morphologies and varying melanin content. The diagnostic process for GI melanoma can become particularly intricate when the tumor lacks melanin pigmentation. It is crucial for clinicians to recognize that melanomas are not universally characterized by dark pigmentation, and pathological diagnosis may transition from poorly differentiated carcinoma to melanoma following immunohistochemical (IHC) investigations [19]. A definitive diagnosis of melanoma relies on an IHC examination demonstrating positive results for S-100 protein, HMB-45, Melan-A, tyrosinase, and neuron-specific enolase [20, 21].

Endoscopy stands as an intuitive and precise diagnostic method for identifying GI diseases. The endoscopic evaluation of GI melanoma lesions typically presents as black plaques or multiple polypoid lesions, exhibiting pigmented or amelanotic characteristics [9, 22]. In assessing melanoma lesions within the GI tract, endoscopy proves to be a dependable tool for gauging the depth of infiltration. However, considering the limited accessibility of the small intestine for endoscopic examination, non-invasive imaging becomes the preferred modality when there is suspicion of tumor infiltration [23].

The most frequently employed imaging modality for investigating GI symptoms was the CT scan. On CT images, GI melanoma typically exhibits homogeneous density on plain scans and manifests as an inhomogeneous mass with moderate to marked enhancement and a polypoid morphology. GI melanomas can be categorized as submucosa-like or primary carcinoma-like tumors [3]. To enhance sensitivity in detecting GI melanoma, an optimal approach involves the utilization of ^{18}F-FDG PET/CT for comprehensive staging of GI melanoma [24, 25]. GI melanoma typically exhibits high ^{18}F-FDG uptake [4, 26, 27]. Reinhardt et al. [28] reported superior diagnostic accuracy of PET/CT compared to CT for detecting melanoma metastases in general, with a particular advantage in detecting visceral melanoma metastases. ^{18}F-FDG PET/CT plays a pivotal role in both identifying and ruling out metastatic sites and in selecting patients for curative-intent surgical resection. Case 1 and Case 2 in our reports had more metastases detected by FDG PET/CT examination, which increased the staging of the tumor. Case 3 was evaluated for efficacy by FDG PET/CT examination and excluded metastases from other sites, crucial for surgical planning. Surgical excision of metastases is recommended when only one or a few disease sites are discernible [29].

Significantly, radionuclide-labeled melanin-targeted agents bear the potential to make valuable contributions to the characterization, staging, and evaluation of treatment responses in melanoma. Some researchers have demonstrated that melanin-targeted PET imaging, utilizing radiotracers like ^{18}F-PFPN and ^{18}F-VLA-4 ($\alpha4\beta1$ integrin), could offer an effective approach for detecting melanoma metastases [30, 31]. Ongoing advancements in molecular imaging technologies and the continual development of novel tracers hold substantial promise for advancing the diagnosis and management of melanoma, ultimately leading to improved patient outcomes and enhanced overall disease management.

Currently, no standardized therapy regimen is established for the treatment of GI melanoma; however, surgical resection stands as the treatment of choice for all patients with resectable melanoma. It is imperative to achieve precise preoperative diagnosis and thoroughly assess the extent of GI metastases, including the identification of extragastrointestinal metastases, in order to make informed decisions regarding patient suitability for surgery and to plan the surgical procedure effectively. Mucosal melanoma is generally recognized as being resistant to chemotherapy [32, 33]. Metastatic mucosal melanoma is linked to elevated morbidity and mortality, resulting in an unfavorable prognosis. Interestingly, tumor morphology appears to play a role in determining prognosis. In a study by Kim et al. [19], which examined the clinical characteristics and survival outcomes of 17 esophageal melanoma patients, it was observed that individuals with a diffusely infiltrative tumor morphology (n = 2) exhibited significantly better overall survival compared to those with mass-forming tumor morphology (n = 15) (P = 0.048).

Immunotherapy has achieved remarkable success in the treatment of cutaneous melanoma [34]. However, prior investigations have documented lower response rates to immunotherapy in mucosal melanoma as compared to cutaneous melanoma. In a comprehensive pooled

analysis of clinical trials conducted by D'Angelo et al. [35], the median progression-free survival for patients receiving Nivolumab monotherapy was 3.0 months for mucosal melanoma and 6.2 months for cutaneous melanoma, respectively. A combination therapy involving Nivolumab and Ipilimumab yielded more favorable outcomes, with a median progression-free survival of 5.9 months for mucosal melanoma and 11.7 months for cutaneous melanoma, respectively. Further extensive studies on a larger scale are imperative to assess the efficacy of immunotherapy in patients with GI melanoma.

Conclusion

In summary, melanoma typically arises in locations where melanocytes are naturally present, such as the skin, eyes, meninges, and anal region, but it can also manifest as a primary tumor within the GI tract. Therefore, melanoma should be included in the differential diagnosis of primary GI malignancies. Vigilant long-term follow-up is imperative to monitor the potential for recurrence and metastasis. In this report, we present three cases that contribute to a deeper comprehension of this disease for clinicians. The ^{18}F-FDG PET/CT examination enables comprehensive visualization of the lesion's location and extent, serving as a foundation for clinical tumor staging and aiding in treatment monitoring and post-treatment follow-up.

Acknowledgements

This work was supported by the National High Level Hospital Clinical Research Fund (Interdisciplinary Research Project of Peking University First Hospital, 2023IR17), National Natural Science Foundation of China (82171970), the Beijing Science Foundation for Distinguished Young Scholars (JQ21025), and the Beijing Municipal Science & Technology Commission (Z221100007422027).

Disclosure of conflict of interest

None.

Address correspondence to: Lei Kang, Department of Nuclear Medicine, Peking University First Hospital, Beijing 100034, China. Tel: +86-10-83575252; E-mail: kanglei@bjmu.edu.cn

References

[1] La Selva D, Kozarek RA, Dorer RK, Rocha FG and Gluck M. Primary and metastatic melanoma of the GI tract: clinical presentation, endoscopic findings, and patient outcomes. Surg Endosc 2020; 34: 4456-62.
[2] Wang S, Ling L, Xu C and Tang G. Primary malignant melanoma of the small intestine. Am J Med Sci 2022; 364: e12-4.
[3] Kohoutova D, Worku D, Aziz H, Teare J, Weir J and Larkin J. Malignant melanoma of the gastrointestinal tract: symptoms, diagnosis, and current treatment options. Cells 2021; 10: 327.
[4] Kaya E, Aksoy T, Güner AL, Temiz H and Vardareli E. Colonic malignant melanoma: 18F-FDG PET/CT findings. Mol Imaging Radionucl Ther 2018; 27: 144-5.
[5] Erdei E and Torres SM. A new understanding in the epidemiology of melanoma. Expert Rev Anticancer Ther 2010; 10: 1811-23.
[6] de Bruin GJ, Mulder AH and Witteman BJ. Primary malignant melanoma of the gastrointestinal tract: a case report and review of the literature. Acta Gastroenterol Belg 2007; 70: 367-70.
[7] Blecker D, Abraham S, Furth EE and Kochman ML. Melanoma in the gastrointestinal tract. Am J Gastroenterol 1999; 94: 3427-33.
[8] Elsayed AM, Albahra M, Nzeako UC and Sobin LH. Malignant melanomas in the small intestine: a study of 103 patients. Am J Gastroenterol 1996; 91: 1001-6.
[9] Wang S, Sun S, Liu X, Ge N, Wang G, Guo J, Liu W and Hu J. Endoscopic diagnosis of gastrointestinal melanoma. Scand J Gastroenterol 2020; 55: 330-7.
[10] McLaughlin CC, Wu XC, Jemal A, Martin HJ, Roche LM and Chen VW. Incidence of noncutaneous melanomas in the U.S. Cancer 2005; 103: 1000-7.
[11] Schaefer T, Satzger I and Gutzmer R. Clinics, prognosis and new therapeutic options in patients with mucosal melanoma: a retrospective analysis of 75 patients. Medicine (Baltimore) 2017; 96: e5753.
[12] Chang AE, Karnell LH and Menck HR. The National Cancer Data Base report on cutaneous and noncutaneous melanoma: a summary of 84,836 cases from the past decade. The American College of Surgeons Commission on Cancer and the American Cancer Society. Cancer 1998; 83: 1664-78.
[13] Lens M, Bataille V and Krivokapic Z. Melanoma of the small intestine. Lancet Oncol 2009; 10: 516-21.
[14] Dalci K, Teke Z, Atar C and Doran F. Primary gastric melanoma presenting with recurrent

upper gastrointestinal bleeding. Ann R Coll Surg Engl 2021; 103: e282-4.
[15] Ozdede M, Guven AT and Yerebakan MB. Relapse of melanoma presenting as jejunal intussusception. Niger J Clin Pract 2023; 26: 365-7.
[16] Mazzeo C, Viscosi F, Foti A and Cucinotta E. Metastatic melanoma of the small bowel. Report of a case and review of literature. Ann Ital Chir 2019; 89: S2239253X19030718.
[17] Parisian KR, Mcfarland JE and Shah AN. Metastatic malignant melanoma of the gastrointestinal tract. Clin Gastroenterol Hepatol 2008; 6: A24-A24, e1.
[18] Khalid U, Saleem T, Imam AM and Khan MR. Pathogenesis, diagnosis and management of primary melanoma of the colon. World J Surg Oncol 2011; 9: 14.
[19] Kim TS, Min BH, Min YW, Lee H, Rhee PL, Kim JJ and Lee JH. Clinical characteristics and treatment outcomes of primary malignant melanoma of esophagus: a single center experience. BMC Gastroenterol 2022; 22: 157.
[20] Cavalaris CP, Okon SO, Pena LR and Friedman MS. Primary malignant melanoma of the esophagus. Dig Dis Sci 2023; 68: 3203-4.
[21] Chu YM, Hung CS and Huang CS. Primary malignant melanoma of the esophagogastric junction: a case report. Medicine (Baltimore) 2021; 100: e26467.
[22] Schuchter LM, Green R and Fraker D. Primary and metastatic diseases in malignant melanoma of the gastrointestinal tract. Curr Opin Oncol 2000; 12: 181-5.
[23] Othman AE, Eigentler TK, Bier G, Pfannenberg C, Bösmüller H, Thiel C, Garbe C, Nikolaou K and Klumpp B. Imaging of gastrointestinal melanoma metastases: correlation with surgery and histopathology of resected specimen. Eur Radiol 2017; 27: 2538-45.
[24] Strobel K, Dummer R, Husarik DB, Pérez Lago M, Hany TF and Steinert HC. High-risk melanoma: accuracy of FDG PET/CT with added CT morphologic information for detection of metastases. Radiology 2007; 244: 566-74.
[25] Patel K, Ward ST, Packer T, Brown S, Marsden J, Thomson M and Ismail T. Malignant melanoma of the gastro-intestinal tract: a case series. Int J Surg 2014; 12: 523-7.
[26] Yen YA, Wu LC, Lu NM and Lee CH. Pigmented villous nodular synovitis mimicking metastases on 18F-FDG PET/CT in a patient with rectal mucosal melanoma: a case report. BMC Musculoskelet Disord 2020; 21: 13.
[27] Jain A, John AR, Kishore B, Vishnoi MG, Pandit AG, Sharma A, Jaimini A, Jain M and Singh A. F-18 fluorodeoxyglucose positron emission tomography/computed tomography in conjunctival melanoma with recurrence. J Cancer Res Ther 2020; 16: S240-2.
[28] Reinhardt MJ, Joe AY, Jaeger U, Huber A, Matthies A, Bucerius J, Roedel R, Strunk H, Bieber T, Biersack HJ and Tüting T. Diagnostic performance of whole body dual modality 18F-FDG PET/CT imaging for N- and M-staging of malignant melanoma: experience with 250 consecutive patients. J Clin Oncol 2006; 24: 1178-87.
[29] Finkelstein SE, Carrasquillo JA, Hoffman JM, Galen B, Choyke P, White DE, Rosenberg SA and Sherry RM. A prospective analysis of positron emission tomography and conventional imaging for detection of stage IV metastatic melanoma in patients undergoing metastasectomy. Ann Surg Oncol 2004; 11: 731-8.
[30] Roxin Á, Zhang C, Huh S, Lepage ML, Zhang Z, Lin KS, Bénard F and Perrin DM. Preliminary evaluation of 18F-labeled LLP2A-trifluoroborate conjugates as VLA-4 (α4β1 integrin) specific radiotracers for PET imaging of melanoma. Nucl Med Biol 2018; 61: 11-20.
[31] Zhang X, Li M and Lan X. Melanin-targeted PET imaging with 18F-PFPN for identifying gastric metastatic melanoma. Clin Nucl Med 2022; 47: 666-7.
[32] Yang AS and Chapman PB. The history and future of chemotherapy for melanoma. Hematol Oncol Clin North Am 2009; 23: 583-97.
[33] Tyrrell H and Payne M. Combatting mucosal melanoma: recent advances and future perspectives. Melanoma Manag 2018; 5: MMT11.
[34] Kaufman HL, Kirkwood JM, Hodi FS, Agarwala S, Amatruda T, Bines SD, Clark JI, Curti B, Ernstoff MS, Gajewski T, Gonzalez R, Hyde LJ, Lawson D, Lotze M, Lutzky J, Margolin K, McDermott DF, Morton D, Pavlick A, Richards JM, Sharfman W, Sondak VK, Sosman J, Steel S, Tarhini A, Thompson JA, Titze J, Urba W, White R and Atkins MB. The Society for Immunotherapy of Cancer consensus statement on tumour immunotherapy for the treatment of cutaneous melanoma. Nat Rev Clin Oncol 2013; 10: 588-98.
[35] D'Angelo SP, Larkin J, Sosman JA, Lebbé C, Brady B, Neyns B, Schmidt H, Hassel JC, Hodi FS, Lorigan P, Savage KJ, Miller WH Jr, Mohr P, Marquez-Rodas I, Charles J, Kaatz M, Sznol M, Weber JS, Shoushtari AN, Ruisi M, Jiang J and Wolchok JD. Efficacy and safety of nivolumab alone or in combination with ipilimumab in patients with mucosal melanoma: a pooled analysis. J Clin Oncol 2017; 35: 226-35.